PNAS RESEARCH ARTICLE | NEUROSCIENCE

Differential modulation of pain and associated anxiety by GABAergic neuronal circuits in the lateral habenula

Teng Chen[a], Wen-Bo Liu[a], Sheng-Jie Zhu[b], Abudula Aji[a], Chen Zhang[a], Chao-Chen Zhang[a], Yu-Jie Duan[c], Jia-Xin Zuo[a], Zhe-Chen Liu[a], Hao-Jun Li[a], Yu-Quan Wang[a], Wen-Li Mi[a], Qi-Liang Mao-Ying[a], Yan-Qing Wang[a,d,1], and Yu-Xia Chu[a,1]

Edited by Hee-Sup Shin, Institute for Basic Science, Daejeon, South Korea; received May 12, 2024; accepted October 20, 2024

Persistent pain frequently precipitates the development of anxiety disorders, yet the underlying mechanisms are not fully understood. In this study, we employed a mouse model that simulates trigeminal neuralgia and observed a marked reduction in the activity of GABAergic neurons in the lateral habenula (LHb), a critical region for modulating pain and anxiety. We utilized precise optogenetic and chemogenetic techniques to modulate these neurons, which significantly alleviated behaviors associated with pain and anxiety. Our investigations revealed an inhibitory pathway from the LHb GABAergic neurons to the posterior paraventricular thalamus. Activation of this pathway primarily mitigated pain-related behaviors, with minimal effects on anxiety. Conversely, interactions between GABAergic and glutamatergic neurons within the LHb were essential in alleviating both pain and anxiety following trigeminal nerve damage. Additionally, we identified that β-sitosterol interacts directly with LHb GABAergic neurons via the estrogen receptor α, providing dual therapeutic effects for both pain and anxiety. These findings highlight the critical role of reduced GABAergic neuronal activity in the LHb in the intersection of pain and anxiety, pointing to promising therapeutic possibilities.

pain | anxiety | neural circuit

Significance

Our study underscores the critical role of GABAergic neurons in the lateral habenula (LHb) in regulating chronic pain and associated anxiety. We identified an inhibitory pathway from these LHb neurons to the posterior paraventricular thalamus that selectively mitigates chronic pain without affecting anxiety. This inhibitory effect also operates within the LHb, providing combined relief from both conditions. Furthermore, the plant sterol β-sitosterol activates these neurons through the estrogen receptor α, introducing a promising dual therapeutic strategy for treating these comorbidities.

Persistent pain is a complex physiological phenomenon that often coexists with significant psychiatric conditions, particularly anxiety, exacerbating clinical challenges (1–3). This co-occurrence not only intensifies the perceived severity and persistence of pain but also complicates clinical interventions, often resulting in suboptimal patient outcomes (4, 5). Such overlap suggests shared neural underpinnings between pain and anxiety. Despite this, a detailed understanding of the neural circuits and molecular mechanisms that underlie their coexistence remains elusive. This gap highlights the urgent need for further investigation to identify potential therapeutic targets.

The lateral habenula (LHb), an evolutionarily conserved brain region, has been increasingly acknowledged for its pivotal role in modulating pain perceptions and a spectrum of negative emotions, including anxiety and depression (6). Historically, the primary functional paradigm of the LHb was believed to center around its glutamatergic neurons (6). Our previous work demonstrated that chemogenetic bilateral inhibition of these neurons significantly reduced pain-like and anxiety-like behaviors in mice following a partial transection of the infraorbital nerve (pT-ION) (7). However, the mechanisms underlying the overactivity of LHb's glutamatergic neurons remain unclear. Recent neurobiological studies have identified a critical subset of GABAergic inhibitory neurons within the LHb. Although less numerous, these neurons influence a range of behaviors, including aggression, motivation, and escape responses (8–10). The projection patterns of these GABAergic neurons are currently debated: Some studies suggest primarily local connections (8), while others propose projections extending to distant regions such as the substantia nigra pars reticulata (9). Generally, GABAergic neurons in the LHb can inhibit the activity of colocalized glutamatergic neurons. Notably, our preliminary results indicate a reduction in GABAergic neuronal activity in the LHb following pT-ION, alongside the emergence of an inhibitory projection from LHb GABAergic neurons to glutamatergic neurons in the posterior paraventricular thalamus (pPVT). This reduction in GABAergic function likely contributes to the overexcitation of glutamatergic neurons within the LHb and diminished GABAergic output to other nuclei, precipitating chronic pain and concurrent anxiety.

Both mood regulation and pain perception are intricately linked with estrogen levels (11, 12). Notably, reductions in estrogen are associated with conditions such as perimenopausal depression (13). During pregnancy, elevated estrogen levels are often correlated with improved mood and decreased pain sensitivity, as reported anecdotally by some expectant individuals (14). Additionally, estrogen deficiencies are linked to the onset of

Author affiliations: [a]Department of Integrative Medicine and Neurobiology, School of Basic Medical Sciences, Shanghai Medical College, Institute of Acupuncture Research, Institutes of Integrative Medicine, Shanghai Key Laboratory of Acupuncture Mechanism and Acupoint Function, Fudan University, Shanghai 200032, China; [b]Department of Dermatology, Yueyang Hospital of Integrated Traditional Chinese and Western Medicine, Shanghai University of Traditional Chinese Medicine, Shanghai 200437, China; [c]School of Rehabilitation Science, Shanghai University of Traditional Chinese Medicine, Shanghai 201399, China; and [d]State Key Laboratory of Medical Neurobiology and Ministry of Education Frontiers Center for Brain Science, Institutes of Brain Science, Fudan University, Shanghai 200032, China

Author contributions: Yan-Qing Wang and Y.-X.C. designed research; T.C., W.-B.L., S.-J.Z., A.A., C.Z., C.-C.Z., J.-X.Z., Z.-C.L., and H.-J.L. performed research; Y.-J.D. and Yu-Quan Wang analyzed data; and T.C., W.-L.M., Q.-L.M.-Y., and Y.-X.C. wrote the paper.

The authors declare no competing interest.

This article is a PNAS Direct Submission.

[1]To whom correspondence may be addressed. Email: wangyanqing@shmu.edu.cn or yuxiachu@fudan.edu.cn.

This article contains supporting information online at https://www.pnas.org/lookup/suppl/doi:10.1073/pnas.2409443121/-/DCSupplemental.

Published November 20, 2024.

migraines, particularly menstrually related migraines, which are influenced by both central and peripheral factors (15). The decline in estrogen during spontaneous menstrual cycles or the hormone-free interval of hormonal treatments is frequently implicated. Prophylactic transdermal estrogen application prior to menstruation can help stabilize estrogen levels, thereby reducing fluctuations and potentially preventing migraines. A deeper understanding of the neurobiological mechanisms underpinning these effects is crucial. Importantly, LHb GABAergic neurons show significant expression of estrogen receptor α (ESRα), both transcriptomically and proteomically, and activation of ESRα leads to the inhibition of these neurons (9). In this context, β-sitosterol—a phytosterol found in vegetable oils and seeds—gains attention. Renowned for its analgesic (16), anxiolytic (17), and antidepressant (18) properties, β-sitosterol's ability to modulate LHb GABAergic neurons through ESRα presents a promising therapeutic avenue, particularly within the context of orofacial pain.

In this study, we aim to elucidate the role of LHb GABAergic neurons in modulating pain and associated anxiety, and to explore potential therapeutic agents. To achieve this, we employed a combination of viral tracing, behavioral testing, and in vitro patch clamp recordings. These methods helped us identify the critical functions of GABAergic circuits both within the LHb (LHb^{GABA}→LHb^{Glu}) and extending to the pPVT (LHb^{GABA}→$pPVT^{Glu}$) in mice suffering from nerve injury-induced orofacial pain and concurrent anxiety. Additionally, we assessed the therapeutic potential of the ESRα agonist, β-sitosterol. Our findings highlight the significant role of LHb GABAergic neurons in mediating the complex interplay between pain and anxiety, thereby suggesting broad avenues for innovative therapeutic interventions.

Results

Alleviation of pT-ION-Induced Pain- and Anxiety-Like Behaviors through Activation of LHb GABAergic Neurons. To assess the activity of LHb GABAergic neurons following pT-ION surgery (Fig. 1*A*), we performed whole-cell patch-clamp recordings on identifiable LHb GABAergic neurons in VGAT-tdTOM mice (refer to Fig. 1*B*). We measured the spontaneous excitatory postsynaptic currents (sEPSCs) in the presence of the $GABA_A$ receptor antagonist, bicuculline (Fig. 1*C*). While the frequency of sEPSCs did not differ significantly from that of the sham-operated controls, their amplitude was reduced in the pT-ION group (Fig. 1*C*), indicating decreased activity of LHb GABAergic neurons. Additionally, the number of action potential spikes induced by 5 pA depolarizing current steps also decreased in these neurons in the pT-ION mice (Fig. 1*D*). These findings collectively indicate a reduction in excitability of LHb GABAergic neurons in the context of orofacial pain.

To investigate the role of LHb GABAergic neurons in modulating pain-like and anxiety-like behaviors, we implemented an optogenetic approach using glutamic acid decarboxylase 2 (GAD2) as a marker for these neurons. In GAD2-Cre mice, we introduced either AAV-DIO-ChR2 (channelrhodopsin) or AAV-DIO-mCherry into the LHb, and implanted an optical fiber above this region (illustrated in Fig. 1 *E*–*G*). Optogenetic stimulation (473 nm, 20 Hz, 5 mw, 20 ms) of LHb GABAergic neurons substantially alleviated primary (V2) and secondary mechanical allodynia (V3), as well as secondary cold allodynia (shown in Fig. 1*H*). Behavioral assessments, including the elevated plus maze (EPM) and open field test (OFT), demonstrated that this stimulation significantly reduced anxiety-like behaviors associated with nerve injury (Fig. 1 *I* and *J*). To further validate the role of these neurons, we employed a chemogenetic strategy in GAD2-Cre mice, introducing AAV-DIO-hM3Dq into the LHb followed by systemic administration of clozapine-N-oxide (CNO) in pT-ION mice (details in *SI Appendix*, Fig. S1 *A*–*C*). This chemogenetic activation replicated the alleviation of pain and anxiety-like behaviors observed with optogenetic stimulation, confirming the modulatory impact of LHb GABAergic neurons on these behaviors (results detailed in *SI Appendix*, Fig. S1 *D*–*F*).

To replicate the observed decrease in LHb GABAergic neuronal activity during episodes of pain and anxiety, we targeted these neurons for inhibition. This was accomplished by introducing AAV-VGAT1-hM4Di into the LHb of C57BL/6 mice, followed by intraperitoneal administration of CNO in the sham-operated group (refer to *SI Appendix*, Fig. S2 *A* and *B*). The chemogenetic suppression of LHb GABAergic neurons resulted in lowered mechanical pain thresholds in both V2 and V3 areas, accompanied by an increased wiping response following acetone exposure (detailed in *SI Appendix*, Fig. S2*C*). Moreover, this suppression led to pronounced anxiety-like behaviors in subsequent OFT and EPM assessments (shown in *SI Appendix*, Fig. S2 *D* and *E*). Collectively, our results underscore the pivotal role of LHb GABAergic neurons in modulating both pain-like and anxiety-like behaviors.

The LHb^{GABA}→pPVT Circuit Modulates Pain-Like Behaviors without Influencing Anxiety-Like Responses. Previous research suggested that the primary projections of LHb GABAergic neurons are confined to local regions (8). To investigate the possibility of their long-distance projections, we utilized anterograde tracing with AAV-DIO-mCherry in the left LHb of GAD2-Cre mice (Fig. 2*A*). Four weeks postinjection, mCherry-positive fibers were observed in the pPVT (Fig. 2*B*), but not in other known LHb target areas such as dorsal raphe nucleus (DRN), median raphe nucleus (MRN), or the ventral tegmental area (VTA) (*SI Appendix*, Fig. S3). We then explored the functional connectivity of the LHb^{GABA}→pPVT pathway by infusing AAV-DIO-ChR2 into the LHb of GAD2-Cre mice and stimulating the pPVT with blue light pulses (473 nm, 20 Hz, 60 μw, 20 ms), while recording from putative pPVT neurons using electrophysiological techniques (Fig. 2*C*). Activation of LHb GABAergic neuron terminals via ChR2 induced optically evoked inhibitory postsynaptic currents (oIPSCs) in approximately 20% of the pPVT neurons at 0 mV (Fig. 2 *D* and *E*). Notably, no excitatory activity was detected when these neurons were held at -70 mV. These findings confirm that GABAergic neurons in the LHb form inhibitory connections with the pPVT.

To investigate the role of the LHb^{GABA}→pPVT pathway in modulating pain and anxiety responses, we injected AAV-DIO-hM3Dq into the LHb of GAD2-Cre mice and positioned a cannula within the pPVT of pT-ION mice (Fig. 2 *F*–*H*). Within 5 min of administering CNO into the pPVT, activation of this pathway via hM3Dq-CNO led to a reduction in both primary and secondary mechanical allodynia, as well as secondary cold allodynia (illustrated in Fig. 2*I*). However, this chemogenetic activation did not significantly alter anxiety-like behaviors, as indicated by outcomes in the OFT and EPM (Fig. 2 *J* and *K*). It is well established that the pPVT predominantly consists of glutamatergic neurons, with a noted absence of GABAergic neurons (19–21). Our immunostaining across multiple layers further confirmed the lack of GABAergic signals within the pPVT, as illustrated in *SI Appendix*, Fig. S4. Additionally, the targeted activation of GABAergic neurons in the LHb of GAD2-Cre mice injected with DIO virus substantiates the exclusion of localized microcircuits within the pPVT from our considerations. These findings underscore the LHb^{GABA}→pPVT pathway's specific influence on pain-related behaviors without affecting anxiety-related responses.

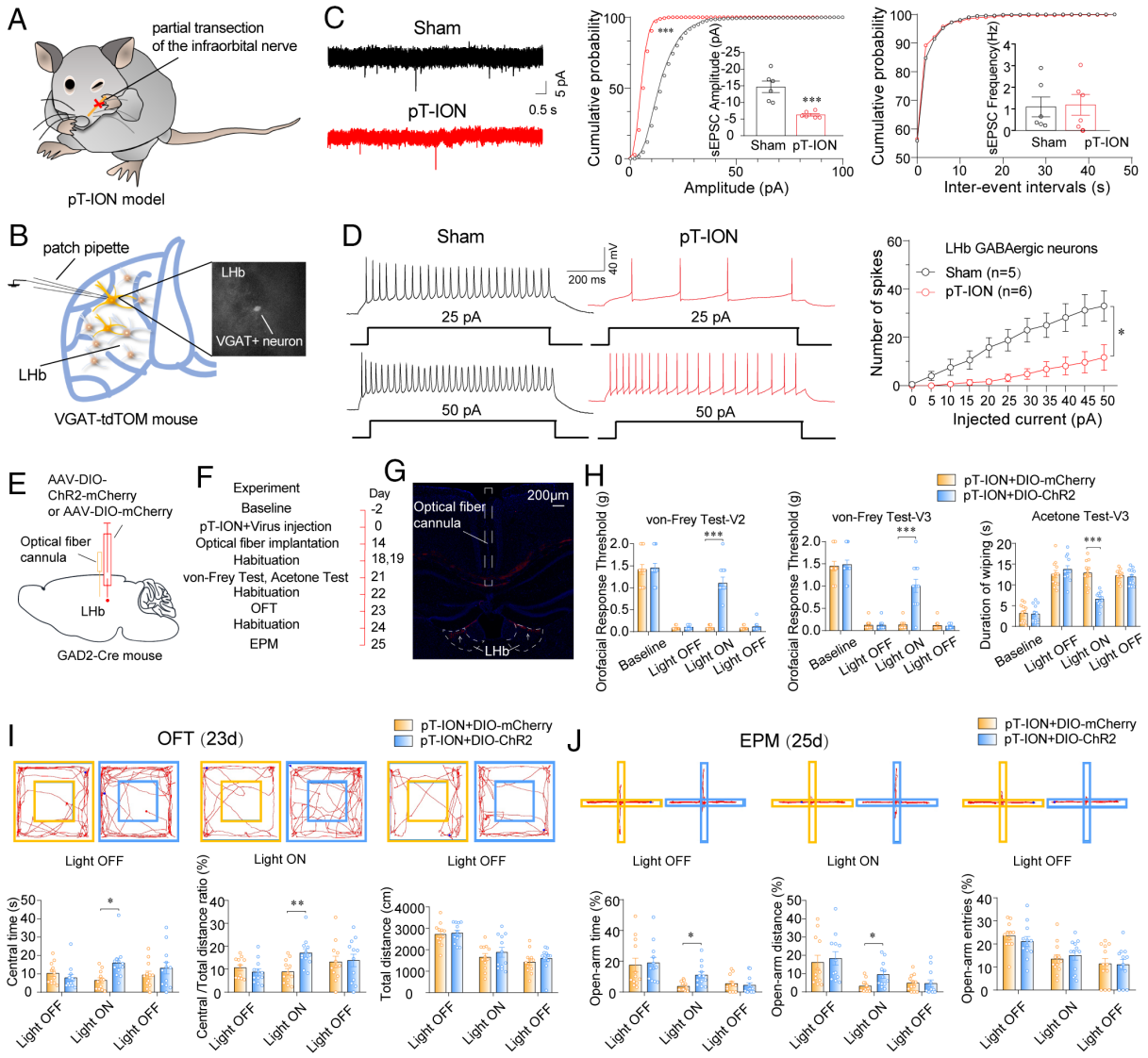

Fig. 1. Optogenetic activation of LHb GABAergic neurons alleviates pain-like and anxiety-like behaviors in pT-ION mice. (*A*) Diagram illustrating the pT-ION mouse model. (*B*) Schematic of the recording setup in acute slices. (*C*) Electrophysiological traces and summarized data from LHb GABAergic neurons in sham and pT-ION groups [two-tailed Student's *t* test, sham, $n = 6$ cells from 6 mice (3♂+3♀); pT-ION, $n = 6$ cells from 6 mice (3♂+3♀); amplitude, $t_{10} = 4.744$, $P = 0.005$; interevent intervals, $t_{10} = 0.1454$, $P = 0.9275$]. (*D*) Traces showing evoked action potentials in LHb GABAergic neurons from sham and pT-ION mice [two-way ANOVA, sham, $n = 5$ cells from 5 mice (3♂+2♀); pT-ION, $n = 6$ cells from 6 mice (3♂+3♀); $F_{1,9} = 10.16$, $P = 0.0111$]. (*E* and *F*) Schematics of surgical procedures and optogenetic stimulation protocol in pT-ION mice. (*G*) Image showing viral delivery for optogenetic targeting of LHb GABAergic neurons. (Scale bar, 200 μm). (*H*) ChR2-mediated stimulation significantly reduced mechanical allodynia in the orofacial V2 and V3 areas, and cold allodynia in the V3 area [two-way ANOVA followed by Sidak's multiple comparisons test, DIO-mCherry, $n = 12$ mice (8♂+4♀); DIO-ChR2, $n = 12$ mice (7♂+5♀); V2: $F_{1.836,40.38} = 141.0$, $P < 0.001$; V3 mechanical: $F_{1.949,42.87} = 164.6$, $P < 0.0003$; V3 cold: $F_{2.294,50.47} = 83.51$, $P < 0.001$]. (*I*) In the OFT, ChR2 stimulation increased the central time and central/total distance ratio, without affecting the total distance (two-way ANOVA followed by Sidak's multiple comparisons test, central time: $F_{2,44} = 0.7464$, $P = 0.0107$; central/total distance ratio: $F_{1.737,\ 38.22} = 2.669$, $P = 0.0064$; total distance: $F_{1.599,\ 35.18} = 37.09$, $P = 0.8180$). (*J*) In the EPM, ChR2 stimulation enhanced the percentage of time and distance in open arms, without altering the percentage of open-arm entries (two-way ANOVA followed by Sidak's multiple comparisons test, time: $F_{1.427,31.40} = 14.07$, $P = 0.0165$; distance: $F_{1.461,\ 32.14} = 13.21$, $P = 0.0325$; entries: $F_{1.966,\ 43.24} = 17.35$, $P = 0.9309$). All data are presented as mean ± SEM. Significance levels: $^*P < 0.05$, $^{**}P < 0.01$, $^{***}P < 0.001$.

Hyperactivity of pPVT Glutamatergic Neurons Underlies Pain-Like Behaviors, Excluding Anxiety-Like Manifestations. To clarify the specific roles of pPVT neurons in modulating pain and anxiety, we first analyzed the activity of pPVT neurons in pT-ION mice. We observed that both the amplitude and frequency of sEPSCs significantly increased in these neurons post-pT-ION surgery (*SI Appendix*, Fig. S5*A*). Furthermore, upon applying 5 pA step depolarizing current pulses, we noted a leftward shift in the input–output curves of these neurons, indicating that the same intensity of current pulse can induce more spikes in the pT-ION group. This was accompanied by a decrease in the rheobase current, suggesting a lower threshold for inducing action potentials (outlined in *SI Appendix*, Fig. S5 *B* and *C*). Additionally, although there was an increase in the resting membrane potential (RMP), the action potential firing threshold remained largely unchanged after surgery (*SI Appendix*, Fig. S5*C*). Collectively, these findings strongly suggest that under neuropathic pain conditions, pPVT neurons exhibit hyperexcitability, contributing specifically to pain-like behaviors without affecting anxiety-like manifestations.

In an effort to further understand the functional implications of pPVT glutamatergic neurons on behavioral responses, we employed AAV-CaMKIIα (a marker for glutamatergic neurons) tagged with hM4Di in pT-ION mice, followed by intraperitoneal administration of CNO (*SI Appendix*, Fig. S5 *D* and *E*). The hM4Di-CNO-mediated inhibition of pPVT resulted in a significant reduction in both primary and secondary mechanical

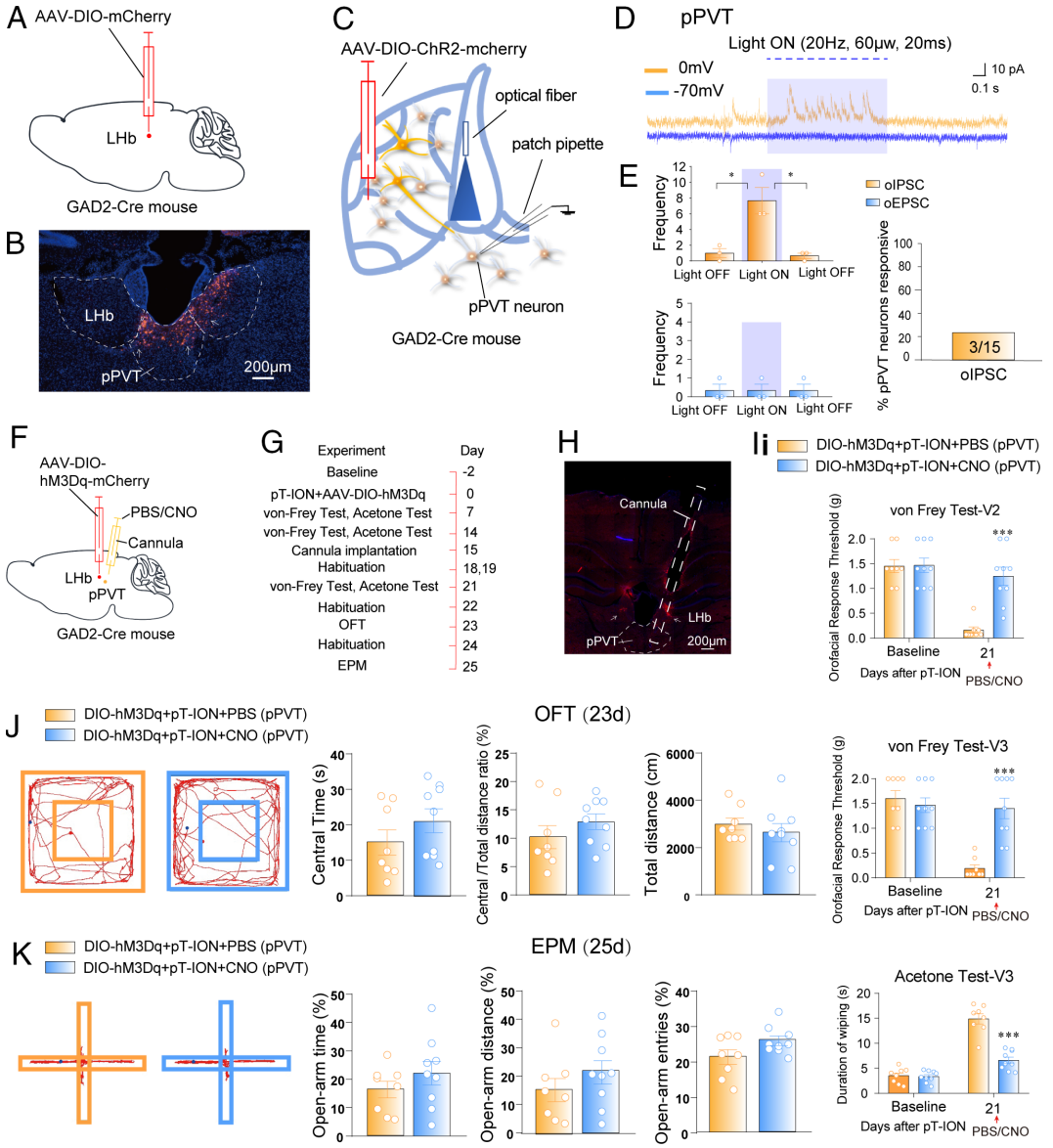

Fig. 2. Activation of LHb^{GABA}→pPVT projections alleviates pain-like but not anxiety-like behaviors in pT-ION mice. (*A* and *B*) Schematic illustration and representative image showing the virus injection site and viral infection for anterograde tracing of LHb GABAergic neurons. (Scale bar, 200 μm). (*C* and *D*) Diagrams of virus injection and fiber-optic placement with sample electrophysiological traces of optically evoked inhibitory postsynaptic currents (oIPSC) and excitatory postsynaptic currents (oEPSC) in pPVT neurons [oIPSC, one-way ANOVA followed by Holm–Sidak's multiple comparisons test, n = 3 neurons from 3 mice (3♂); $F_{2,4}$ = 15.04, Light OFF(Pre) vs. Light ON, P = 0.0168, Light OFF(Post) vs. Light ON, P = 0.0142; oEPSC, one-way ANOVA followed by Holm–Sidak's multiple comparisons test, $F_{2,6}$ = 1.00, Light OFF(Pre) vs. Light ON, P > 0.9999, Light OFF(Post) vs. Light ON, P > 0.9999]. (*E*) Data summarizing the frequency and proportion of pPVT neurons responsive to optogenetic stimulation of LHb GABAergic neurons. (*F* and *G*) Surgical illustrations and experimental setup for chemogenetic activation of LHb GABAergic neuron terminals in the pPVT of pT-ION mice. (*H*) Representative image showing viral infection for in vivo chemogenetic studies on LHb GABAergic neurons. (Scale bar, 200 μm). (*I*) hM3Dq-CNO-mediated stimulation significantly reduced mechanical allodynia in the orofacial V2 and V3 areas, and cold allodynia in the V3 area [two-way ANOVA followed by Sidak's multiple comparisons test, PBS, n = 8 mice (5♂+3♀); CNO, n = 9 mice (6♂+3♀); V2: $F_{1,15}$ = 18.94, P < 0.0001; V3 mechanical: $F_{1,15}$ = 14.45, P < 0.0001; V3 cold: $F_{1,15}$ = 44.38, P < 0.0001]. (*J* and *K*) Chemogenetic stimulation did not significantly affect anxiety-related measures in the OFT or EPM (two-tailed Student's t test, OFT: central time, t_{15} = 1.256, P = 0.2282; central/total distance ratio, t_{15} = 1.129, P = 0.2766; total distance, t_{15}= 0.7639, P = 0.4568; EPM: open-arm time percentage, t_{15} = 1.113, P = 0.2834; open-arm distance percentage, t_{15} = 1.066, P = 0.3033; open-arm entries percentage, t_{15} = 1.920, P = 0.0741). All data are presented as mean ± SEM. Significance levels: *P < 0.05, ***P < 0.001.

allodynia, as well as secondary cold allodynia (*SI Appendix*, Fig. S5*F*). However, this chemogenetic modulation of pPVT did not notably alter anxiety-related behaviors, as evidenced in the OFT and EPM tests (*SI Appendix*, Fig. S5 *G* and *H*). Complementarily, activation of pPVT via AAV-CaMKIIα-hM3Dq, followed by CNO administration in sham-controlled mice, induced clear signs of both mechanical and cold allodynia (*SI Appendix*, Fig. S6 *A–D*), but failed to produce significant changes in anxiety-related behaviors (*SI Appendix*, Fig. S6 *E* and *F*). Additionally, when hM4Di-CNO was used to inhibit the pPVT in sham samples, behaviors related to pain and anxiety remained largely unchanged (*SI Appendix*, Fig. S7). Collectively, these findings underscore the predominant role of pPVT in mediating pain-related behaviors, while its impact on anxiety-related behaviors appears to be minimal.

The LHb^{GABA}→LHb^{Glu} Circuit Ameliorates Both Pain- and Anxiety-Like Behaviors. In previous studies, we demonstrated that chemogenetic inhibition of LHb glutamatergic neurons reduced both pain and anxiety behaviors (7). Extending these findings, we introduced AAV-CaMKIIα-ChR2 or AAV-CaMKIIα-EYFP into the LHb and positioned an optical fiber above this region in sham

control animals (Fig. 3 *A* and *B*). Optogenetic activation of these glutamatergic neurons (473 nm, 20 Hz, 5 mw, 20 ms) induced mechanical and cold allodynia in sham-controlled subjects (Fig. 3*C*), and triggered anxiety-related behaviors, as evidenced by results from the OFT and EPM tests (Fig. 3 *D* and *E*). To further elucidate the interactions within the LHb^{GABA}→LHb^{Glu} circuit, we introduced AAV-DIO-ChR2 into the LHb of GAD2-Cre mice and activated these neurons using blue light (473 nm, 20 Hz, 60 μw, 20 ms) while recording electrophysiological data from presumed non-GAD2 expressing LHb glutamatergic neurons (Fig. 3*F*). This approach revealed that ChR2-mediated stimulation of LHb GAD2-positive neurons generated oIPSCs in approximately 20% of LHb glutamatergic neurons (Fig. 3 *G–I*). Notably, optically evoked excitatory postsynaptic currents (oEPSCs) were absent in the local LHb glutamatergic neurons. Collectively, these findings suggest that LHb GABAergic neurons establish inhibitory synaptic connections with neighboring glutamatergic neurons, influencing both pain and anxiety behaviors.

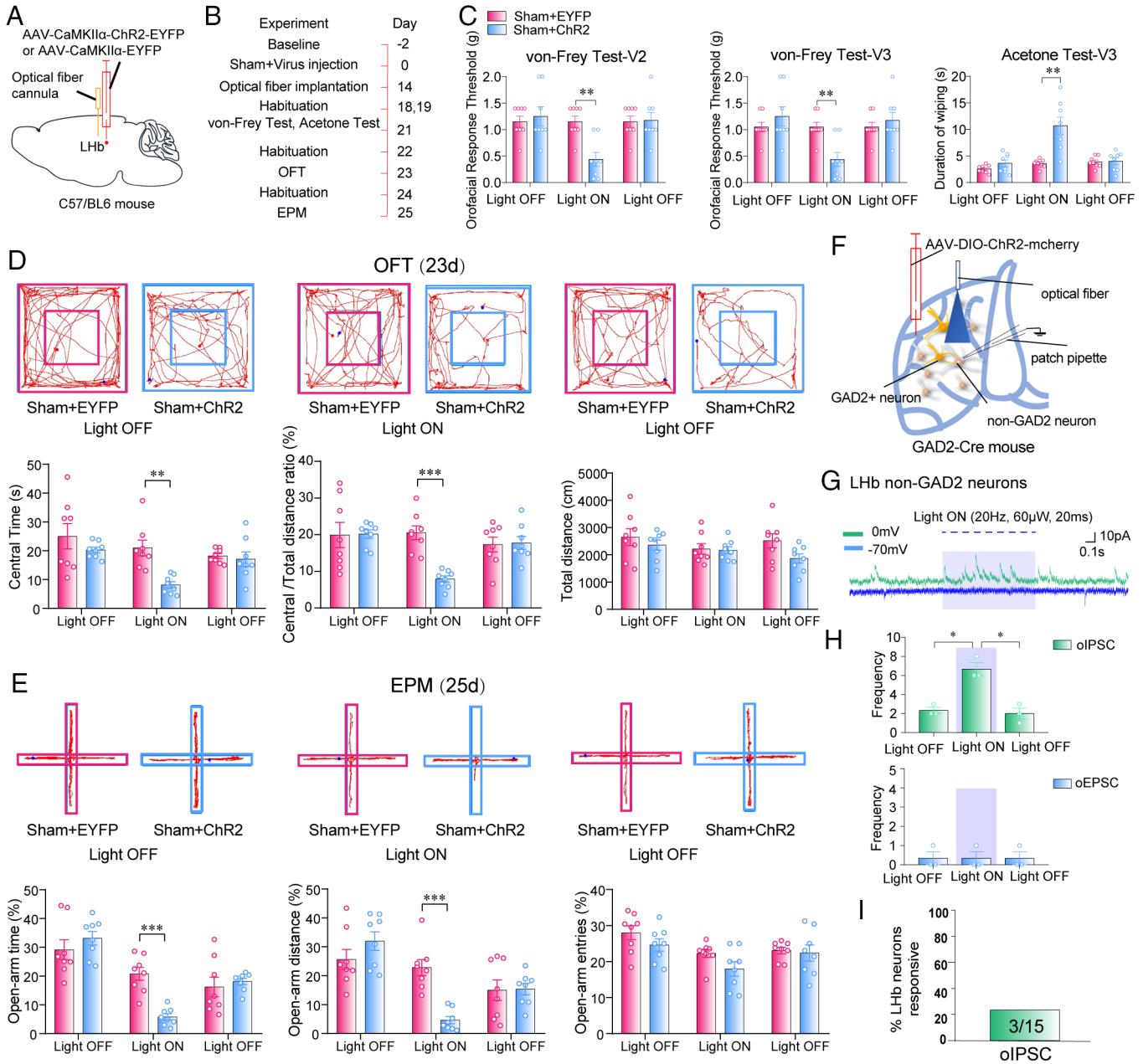

Fig. 3. Optogenetic activation of LHb glutamatergic neurons induces pain-like and anxiety-like behaviors in sham mice. (*A* and *B*) Schematic depiction of virus injection, fiber-optic implantation sites, and the experimental design for optogenetic activation of LHb glutamatergic neurons in sham mice. (*C*) Activation via ChR2 in LHb glutamatergic neurons triggered mechanical allodynia in the orofacial V2 [two-way ANOVA followed by Sidak's multiple comparisons test, EYFP, $n = 8$ mice (8♂); ChR2, $n = 8$ mice (8♂); $F_{1,14} = 1.320$, $P = 0.0029$] and V3 areas ($F_{1,14} = 0.3504$, $P = 0.0070$), and cold allodynia in the V3 area ($F_{1,14} = 18.05$, $P = 0.0094$). (*D*) This optogenetic activation also resulted in a decrease in central time ($F_{1,14} = 8.481$, $P = 0.0049$) and central/total distance ratio ($F_{1,14} = 4.270$, $P = 0.0004$) in the OFT, while total distance remained unaffected ($F_{1,14} = 4.336$, $P = 0.9968$). (*E*) In the EPM, ChR2 activation reduced open-arm time percentage ($F_{1,14} = 2.083$, $P = 0.0004$) and open-arm distance percentage ($F_{1,14} = 3.407$, $P = 0.0004$), but did not significantly alter open-arm entries percentage ($F_{1,14} = 2.608$, $P = 0.2353$). (*F* and *G*) Diagram of experimental operations and sample traces of oIPSC and oEPSC from LHb glutamatergic neurons. (*H* and *I*) Data detailing the frequency and proportion of LHb glutamatergic neurons responding to optogenetic activation of LHb GABAergic neurons (oIPSC, one-way ANOVA followed by Holm–Sidak's multiple comparisons test, n = 3 neurons from 3 mice (3♂); $F_{2,4} = 15.04$, Light OFF(Pre) vs. Light ON, $P = 0.0390$, Light OFF(Post) vs. Light ON, $P = 0.0101$; oEPSC, one-way ANOVA followed by Holm–Sidak's multiple comparisons test, $F_{2,6} = 1.00$, Light OFF(Pre) vs. Light ON, $P > 0.9999$, Light OFF(Post) vs. Light ON, $P > 0.9999$]. All data are presented as mean ± SEM. Significance levels: $^*P < 0.05$, $^{**}P < 0.01$, $^{***}P < 0.001$.

In our subsequent experiments, we sought to elucidate the effects of precisely modulating the LHb^{GABA}→LHb^{Glu} circuit on pain and anxiety manifestations. Due to technical limitations inherent in optogenetic and chemogenetic tools, specifically activating LHb GABAergic terminals without inadvertently affecting the neuronal cytosol—and thereby influencing projections to pPVT's glutamatergic neurons—has been challenging. To overcome this, we developed a refined approach: chemogenetically stimulating LHb GABAergic neurons while simultaneously blocking LHb^{GABA}→pPVT projections with bicuculline (2 μM) introduced into the pPVT of pT-ION subjects. This targeted manipulation of the LHb^{GABA}→LHb^{Glu} pathway resulted in the alleviation of primary and secondary mechanical allodynia, as well as secondary cold allodynia in pT-ION specimens (*SI Appendix*, Fig. S8 *A–C*). Additionally, this precise circuit engagement significantly reduced anxiety-related behaviors, as observed in both the OFT and EPM assessments (*SI Appendix*, Fig. S8 *D* and *E*). Collectively, these findings underscore the significant regulatory role of the LHb^{GABA}→LHb^{Glu} circuit in modulating pain and anxiety-related behaviors.

Direct Modulation of GABAergic Neurons in the LHb by β-Sitosterol Induces Both Analgesic and Anxiolytic Effects. Previous studies have shown significant expression of ESRα in LHb GABAergic neurons (9). Intriguingly, β-sitosterol, known as an ESRα agonist, possesses analgesic, anxiolytic, and antidepressant properties (16–18). Given these properties, we hypothesized that β-sitosterol modulates LHb GABAergic neurons via ESRα, thereby reducing pain- and anxiety-related behaviors in the pT-ION model. To explore this, we administered β-sitosterol intraperitoneally at various concentrations to pT-ION mice. The therapeutic effects of β-sitosterol were evident within an hour after administration, with sustained efficacy for over 10 h, as measured by the von Frey Test (*SI Appendix*, Fig. S9*A*). Doses of β-sitosterol (10, 30, 100 mg/kg) effectively reduced both mechanical and cold allodynia. Notably, the highest dose (100 mg/kg) significantly diminished anxiety-related behaviors in the OFT and EPM (*SI Appendix*, Fig. S9 *B* and *C*). Motor functions remained intact, as confirmed by the Rotarod test (*SI Appendix*, Fig. S10 *A* and *B*).

In our ongoing research, we aimed to determine whether the analgesic and anxiolytic effects of β-sitosterol are mediated through its modulation of ESRα on LHb GABAergic neurons. Using brain slices from VGAT-tdTOM mice with a focus on the LHb, we applied 5 pA step depolarizing currents to induce action potentials. The presence of β-sitosterol in the bath solution significantly increased the number of action potentials within these neurons, an effect that was reversed by the ESRα inhibitor, AZD9496 (Fig. 4 *A–D*), indicating a direct modulatory role of β-sitosterol via ESRα. Further exploring the in vivo impact, we microinjected β-sitosterol directly into the LHb of pT-ION mice using a preset cannula (*SI Appendix*, Fig. S10 *C* and *D*). Remarkably, within 5 min postinjection, there was a significant reduction in both mechanical and cold allodynia (Fig. 4*E*). This intervention also demonstrated anxiolytic effects in subsequent OFT and EPM evaluations (Fig. 4 *F* and *G*). Importantly, rotarod tests confirmed that motor functions were not compromised in pT-ION subjects (*SI Appendix*, Fig. S10*E*). Collectively, these results highlight β-sitosterol's efficacy in alleviating pain and anxiety by targeting ESRα on LHb GABAergic neurons.

Discussion

The LHb is predominantly composed of glutamatergic neurons, known for their heightened activity during pain and adverse emotional states, which are central to the neuropathology of pain and related psychiatric disorders such as anxiety (7) and depression (22, 23). Moving beyond this traditional focus, our multidisciplinary research examines the less studied GABAergic neurons of the LHb. We demonstrate that these neurons play a significant role in regulating these complex physiological and emotional responses. Dysfunctions in GABAergic neuronal activity are notably linked to the simultaneous occurrence of pain and anxiety. These neurons modulate pain and anxiety through both local interactions with glutamatergic neurons and long-range projections to the paraventricular nucleus of the thalamus (pPVT), presenting a multifaceted influence on these states. Furthermore, the positive response of these neurons to the ESRα agonist β-sitosterol highlights a promising avenue for therapeutic interventions targeting this specific neural pathway.

The capability for long-range projections by the LHb GABAergic neurons remains a topic of debate in contemporary neuroscience. Through anterograde virus tracing, our research establishes that these neurons project to the pPVT, confirming their ability to form long-distance connections. This finding stands in contrast to observations by Dr. Russo, who suggested that LHb GAD2 neurons are predominantly localized (8). We hypothesize that the observed discrepancy in the connectivity of LHb GAD2 neurons between our study and Dr. Russo's work may be attributed to two key factors: First, different serotypes of the AAV virus were employed for anterograde tracing. Dr. Russo's group utilized AAV2-DIO-eYFP, whereas our study employed AAV2/9-DIO-mCherry. The AAV2/9 hybrid vectors have demonstrated up to 5 to 100 times higher transgene delivery efficiency compared to AAV2 in the brain (24). Additionally, AAV9 is reported to be more efficient retrograde and anterograde axonal transport and distal transduction (25). Moreover, AAV9 tends to achieve higher expression levels in inhibitory neurons compared to AAV2 (26). Thus, the hybrid AAV2/9 vectors are likely to achieve more potent distal expression at the axon terminals of inhibitory $GAD2^+$ neurons in the LHb. Second, the genetic background of the mice may influence the transduction properties of AAV serotypes in the brain. A study has revealed significant differences in cellular tropism and transduction efficiency among AAV serotypes and between mouse strains, including contralateral transduction (27). It also noted a loss of NeuN-immunoreactivity and microglial activation following AAV transduction across different mouse strains. In Dr. Russo's study, homozygous GAD2-Cre mice were crossed with wild-type CD1 mice, while our study involved crossing homozygous GAD2-Cre mice with wild-type C57BL6 mice. CD1 mice are an outbred strain known for their high genetic diversity, whereas C57BL/6J mice are an inbred strain with a highly uniform genetic background. This variance between the strains could significantly contribute to the discrepancies observed.

Our current findings indicate that hyperactivity of the pPVT in response to trigeminal nerve injury significantly contributes to the development of chronic pain in pT-ION mice. However, chemogenetic inhibition of the pPVT in sham mice did not affect anxiety- or pain-like behaviors, suggesting that pPVT's role in pain modulation is pronounced primarily under conditions of substantial activation rather than its basal activity. In terms of anxiety-like behaviors, neither inhibition nor activation of the pPVT altered behaviors in sham mice, indicating that the pPVT does not contribute to anxiety-like behaviors under normal physiological conditions. Additionally, chemogenetic inhibition of the pPVT did not alleviate pain-associated anxiety-like behaviors in pT-ION mice, as shown in Fig. 3. While previous studies have linked the pPVT to mediating anxiety-like behaviors following acute or repeated stress (28, 29), our results suggest that the pPVT is neither necessary nor sufficient for generating anxiety-like behaviors in either physiological or chronic pain settings.

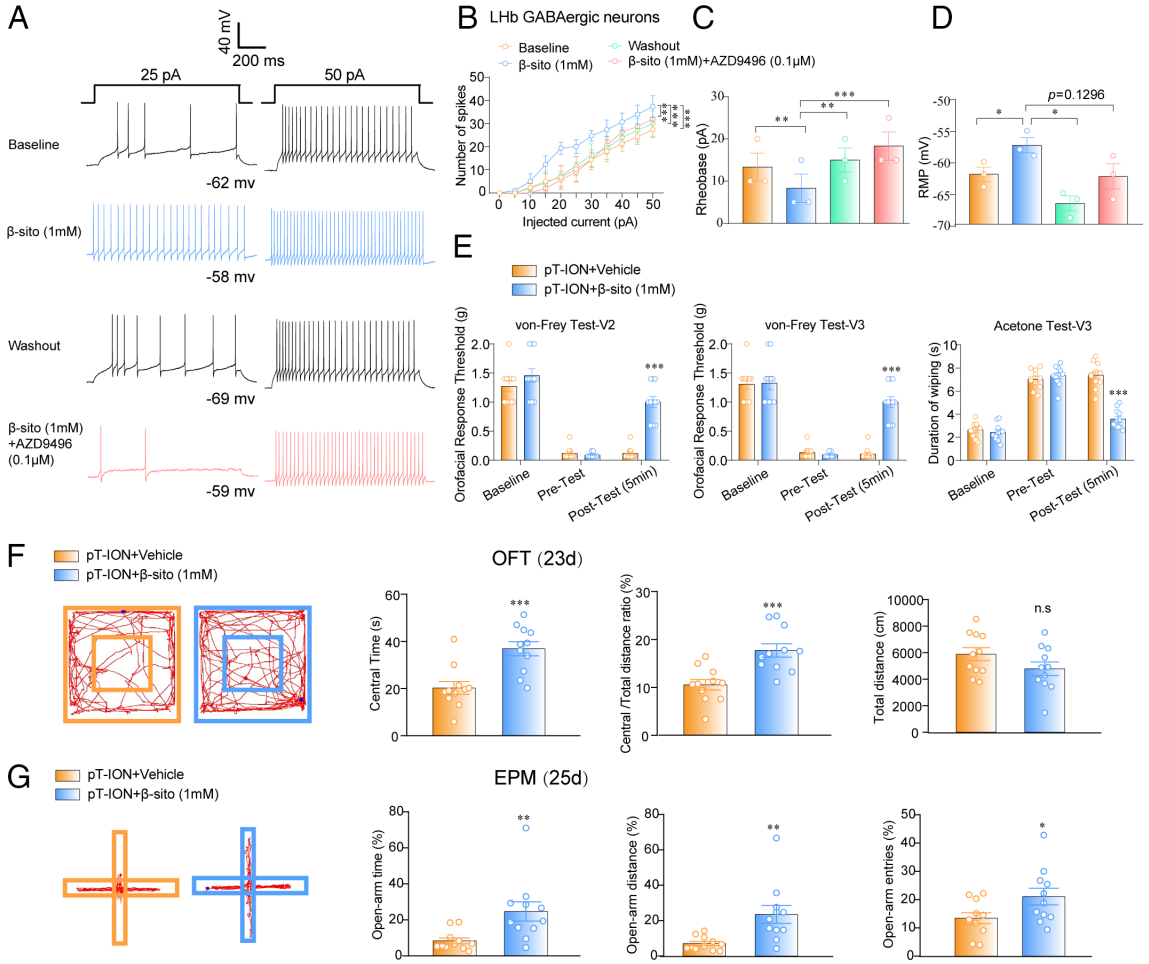

Fig. 4. β-sitosterol alleviates pain-like and anxiety-like behaviors by directly activating LHb GABAergic neurons in pT-ION mice. (*A*) Sample electrophysiological traces show the effects of β-sitosterol, both alone and combined with the ESRα antagonist AZD9496, on LHb GABAergic neurons in acute slices from pT-ION mice. (*B–D*) Application of β-sitosterol resulted in increased spike frequency [Two-way ANOVA followed by Dunnett's multiple comparisons test, n = 3 neurons from 3 mice (3♂); $F_{3,88}$ = 9.830; β-sitosterol vs. Baseline, P < 0.0001; β-sitosterol vs. Washout, P = 0.003; β-sitosterol vs. β-sitosterol+AZD9496, P = 0.001], a decreased rheobase (One-way ANOVA followed by Holm–Sidak's multiple comparisons test, $F_{3,6}$ = 25.00; β-sitosterol vs. Baseline, P = 0.0054; β-sitosterol vs. Washout, P = 0.0026; β-sitosterol vs. β-sitosterol+AZD9496, P = 0.0004), and a shifted RMP ($F_{1.126,2.252}$ = 9.081; β-sitosterol vs. Baseline, P = 0.0151; β-sitosterol vs. Washout, P = 0.0321; β-sitosterol vs. β-sitosterol+AZD9496, P = 0.1296), and (*E*) direct microinjection of β-sitosterol into the LHb significantly reduced mechanical and cold allodynia in the orofacial V2 and V3 areas [two-way ANOVA followed by Sidak's multiple comparisons test, Vehicle, n = 11 mice (11♂); β-sitosterol, n = 11 mice (11♂); V2: $F_{1,20}$ = 28.30, P < 0.0001; V3: $F_{1,20}$ = 22.15, P = 0.0010; cold allodynia: $F_{1,20}$ = 31.75, P < 0.0001]. (*F*) This intervention also increased central time and the ratio of central to total distance in the OFT (two-tailed Student's t test, central time: t_{20} = 4.117, P = 0.0005; central/total distance ratio: t_{20} = 4.027, P = 0.0007), while the overall distance remained unchanged (t_{20} = 1.564, P = 0.1335). (*G*) In the EPM, microinjection of β-sitosterol enhanced the percentage of time spent in the open arms, distance traveled in the open arms, and entries into the open arms (two-tailed Student's t test, time: t_{20} = 2.930, P = 0.0083; distance: t_{20} = 3.176, P = 0.0048; entries: t_{20} = 2.177, P = 0.0416). All data are presented as mean ± SEM. Significance levels: *P < 0.05, **P < 0.01, ***P < 0.001.

Our current and previous research (7, 30) indicates that projections from both pPVT and LHb pyramidal neurons are essential and sufficient for mediating mechanical and cold allodynia. This evidence underscores the necessity and sufficiency of the PVT and LHb in these pain responses, suggesting the potential existence of overlapping pathways or shared downstream targets that modulate these conditions. The central amygdala (CeA), often referred to as the "nociceptive amygdala", is pivotal in processing pain-related information (31). It receives dense projections from the pPVT and is connected via descending nociceptive facilitation pathways implicated in the development of neuropathic pain (32). Additionally, the CeA projects to the LHb, with this pathway mediating depression-like behaviors in chronic pain conditions (22). Moreover, the Ventrolateral Periaqueductal Gray (vlPAG), essential for descending pain modulation, is targeted by the pPVT-CeA pathway, underscoring its role in chronic pain mechanisms (32, 33). Interaction between glutamatergic neurons in the pPVT and GABAergic neurons in the vlPAG can be modulated through chemogenetic and optogenetic techniques to either prevent or induce mechanical allodynia in mice (34). Additionally, the LHb's projections to the vlPAG also influence pain processing, illustrating the complex interplay within these regions (35–37). These insights underscore the interconnected and collaborative nature of the neural circuits involved, suggesting that these regions do not operate in isolation but rather in concert to mediate the full spectrum of pain responses.

The identification of GABAergic neurons in the LHb as modulators of pain and anxiety through distinct neural circuits offers profound physiological and therapeutic insights. This challenges the prevailing hypothesis of a unified neurological pathway for pain and associated negative moods (38), suggesting instead the evolution of separate systems tailored to handle these experiences independently. Such segregation likely interacts with other key neurotransmitter systems (39), including the serotonergic, dopaminergic, and noradrenergic pathways known for their roles in mood regulation and pain modulation. These interactions may clarify the complex clinical presentations often observed (40). The finding of specialized circuits highlights the brain's additional

strategies to counteract the effects of pain and anxiety, underscoring the importance of such redundancy for maintaining homeostasis amid physical and psychological stresses. Clinically, the recognition of these distinct circuits could revolutionize therapeutic approaches, facilitating the development of targeted treatments and enhancing diagnostic precision. Moreover, this understanding could unveil the foundational mechanisms behind conditions like neuropathic pain and generalized anxiety disorders, paving the way for innovative, circuit-specific therapeutic interventions.

Estrogen, the primary female sex hormone, plays critical roles in modulating mood and pain. Studies highlight its analgesic effects, suggesting involvement in the inactivation of kappa opioid receptor signaling, thus mediating analgesia (41). Estrogen's impact on mood is significant across genders. In females, fluctuations in estrogen levels, particularly during the menopausal transition, are associated with an increased risk of mood disorders. Hormone therapies, especially transdermal estradiol, provide potential preventive or therapeutic options for these disturbances. Although the exact mechanisms are not fully understood, the prevailing evidence underscores estrogen's neuromodulatory and neuroprotective roles that affect mood trajectories, facilitated by neural regions rich in estrogen receptors that regulate neurotransmitters. For males, estrogen significantly influences behaviors such as motivation, mood, and anxiety (42), with ESRα playing a key role in delineating sex-specific brain functions, affecting mood and behavior across genders (43). Concurrently, β-sitosterol, a widely recognized phytosterol (44), has been noted for its anxiolytic properties (17). Our research illuminates its interaction with LHb GABAergic neurons via ESRα, highlighting its analgesic and anxiolytic effects. This suggests a reevaluation of β-sitosterol's therapeutic potential, particularly for managing pain and anxiety concurrently. Notably, our findings reveal the therapeutic potential of LHb GABAergic neurons, further supported by the expression of the orexin receptor (8), providing a broad avenue for interventions in pain and anxiety. Given that our study utilized male subjects, our results also suggest the effectiveness of β-sitosterol in managing pain and anxiety across genders.

Extensive prior research has documented the expression of ESRα across both GABAergic and glutamatergic neurons within the LHb (9, 45, 46). Consequently, β-sitosterol's activation of glutamatergic neurons via ESRα cannot be entirely ruled out. However, in another project related to ESRα, we observed a significant decrease in ESRα expression in glutamatergic neurons post-pT-ION injury compared to sham conditions, potentially reducing β-sitosterol's effectiveness on these neurons. Notably, β-sitosterol's robust activation of GABAergic neurons through ESRα may suppress glutamatergic neuron activation both in the LHb and the paraventricular nucleus of the pPVT. This interaction plays a critical role in alleviating both pain-like and anxiety-like behaviors observed in our study. Further research is essential to fully understand the intricate interactions among β-sitosterol, ESRα, and various neuronal types within the LHb.

Our study has revealed critical mechanisms within the LHb, yet it is essential to acknowledge certain limitations. First, while assessing the impact of GABAergic terminal stimulation on glutamatergic neurons in the LHb through patch-clamp recordings is direct, determining behavioral outcomes solely from terminal activation—excluding other cellular activities—poses a significant challenge. In response, we provided indirect evidence by inhibiting the LHb^{GABA}→pPVT pathway using a $GABA_A$ receptor antagonist, a common methodological hurdle in neuroscience. We anticipate that future technological advancements will likely overcome this limitation. Ongoing research is needed to delineate the specific subtypes of LHb GABAergic neurons that modulate pain and associated anxiety. Additionally, while our research primarily utilizes rodent models, which are invaluable, the direct application of these findings to human physiology must be approached with caution. Interspecies differences may affect the relevance of our results to human conditions, necessitating further validation.

In summary, our study reveals that GABAergic neurons in the LHb modulate chronic pain and related anxiety through distinct intranuclear and extranuclear downstream pathways. Additionally, β-sitosterol activates these neurons by interacting with ESRα, providing analgesic and antianxiety benefits, as detailed in *SI Appendix*, Fig. S11. These findings enhance our understanding of the complex neural interactions between pain and anxiety, informing the development of targeted therapeutic strategies for these comorbid conditions.

Materials and Methods

Animals. We obtained male C57BL/6J mice, aged 7 wk, from the Experimental Animal Center of the Chinese Academy of Sciences in Shanghai, China. Heterozygous GAD2-Cre transgenic mice were kindly provided by Dr. Yi-Qun Wang in Fudan University. We crossbred these GAD2-Cre transgenic male mice with wild-type C57BL/6J females to produce offspring with characterized phenotypes. The VGAT-tdTOM mice were generated by crossing VGAT-cre mice with Ai9-tdTOM mice, both of which were originally obtained from the Jackson Laboratory. Our experiments included both male and female GAD2-Cre and VGAT-tdTOM mice, all of which underwent genotype verification. For behavioral assessments and viral tracing studies, we used GAD2-Cre mice aged 8 to 10 wk. Electrophysiological evaluations were performed on GAD2-Cre and VGAT-tdTOM mice aged 5 to 7 wk. Mice were housed in groups of five per cage under controlled conditions with temperatures of 22 ± 1 °C, humidity of 50% to 60%, and a 12-h light–dark cycle (7:00 to 19:00). All mice had ad libitum access to food and water. All procedures involving animals were conducted in strict accordance with the guidelines of the Animal Care and Use Committee at Fudan University and met the standards set by the International Association for the Study of Pain.

Mice Model of the Partial Transection of the Infraorbital Nerve (pT-ION). Mice were anesthetized with 1.25% avertin (sourced from Aladdin), administered intraperitoneally at a dosage of 0.6 mL per 20 g of body weight. A 5 mm incision was made in the buccal mucosa on the left side of each mouse to expose the oral cavity. Using a specialized glass rod for precise dissection, the deeper portion of the infraorbital nerve was gently isolated. This section of the nerve was then securely ligated with sterile catgut, and approximately 2 to 3 mm of the distal segment was excised. The incision was closed using tissue adhesive. Control, or "sham", mice underwent the same procedure for nerve exposure but without the dissection or any subsequent manipulations. Postprocedure, mice were allowed to recover on a warming mat to ensure proper thermoregulation.

Evaluation of Pain-Related Behaviors. Prior to behavioral assessments, mice were acclimatized to the testing environment for 1 d to minimize stress-related variables. The environment was maintained quietly with a temperature of 22 ± 1 °C, humidity between 50% and 60%, and a light intensity of approximately 20 lx. The evaluator was blinded to the group allocation of each mouse to prevent bias.

von-Frey test. Mice underwent a 15-min habituation period on the day preceding testing, during which they were allowed to rest comfortably in the experimenter's gloved hand. For testing, von Frey filaments of varying weights (0.02 g to 2.0 g; sourced from Stoelting) were applied to the facial V2 or V3 region. A positive behavioral response was recorded if the mouse retracted its head upon bending of the filament, maintained for at least 1 s. The lightest filament that elicited three positive responses out of five applications was identified as the orofacial response threshold. Mice demonstrating a lowered response threshold were assessed for mechanical allodynia.

Acetone test. A 0.05 mL volume of acetone was applied to the left V3 region using a Hamilton microsyringe. The duration of face-wiping behavior was observed and recorded over a 2-min period following acetone application. An increased duration of wiping was indicative of cold allodynia.

Assessment of Anxiety-Like Behaviors. Mice were acclimated to the testing environment, which was maintained quiet, with a temperature of 22 ± 1 °C, humidity at 50% to 60%, and light intensity of approximately 20 lx, for 1 d prior to testing. The experimenter was blind to the group assignments to ensure unbiased observations.

OFT. Mice were allowed to explore freely in an open box measuring 50 cm × 50 cm × 40 cm, which included a central area of 25 cm × 25 cm, for a period of 5 min. The time spent and distance traveled in the central area, as well as the total distance, were recorded using a video tracking system (Shanghai Mobile Data Information Technology). The central to total distance ratio was calculated as follows: Central Distance/Total Distance × 100%. The arena was sanitized with 75% ethanol between tests to eliminate olfactory cues.

EPM. In this test, mice were allowed to move freely in a maze comprising a central platform (6 cm × 6 cm), two closed arms (30 cm × 6 cm × 20 cm), and two open arms (30 cm × 6 cm), set 40 cm above the floor. The maze was explored for 5 min. Open-arm time (%) and open-arm distance (%) were quantified as the percentage of total time and total distance in the open arms, respectively. Open-arm entries (%) were calculated as the number of entries into the open arms divided by the total entries into all arms and the central platform, multiplied by 100%. The apparatus was cleaned with 75% ethanol after each session to ensure no residual scents influenced subsequent tests.

Motor Function Evaluation. Rotarod performance test. Mice were acclimatized to the rotarod apparatus (Med Associates) through a training session conducted the day before the actual test, involving three trials. On the test day, the duration each mouse managed to stay on the rotating rod was timed until the mouse fell, with the cut-off time set at 5 min. The apparatus was set to a constant speed of 20 rpm. After each trial, the rotarod was cleaned with a 75% ethanol solution to ensure hygiene and consistency in test conditions.

In Vivo Chemogenetic Manipulations. To specifically target the LHb^{GABA}→pPVT pathway, we bilaterally infused rAAV-Ef1α-DIO-hM3D(Gq)-mCherry-WPRE-pA (AAV-DIO-hM3Dq-mCherry, AAV2/9, 5.36 × 10^{12} vg/mL, 150 nL) into the LHb at coordinates AP −1.62 mm, ML ±0.45 mm, and DV −2.85 mm. For modulating LHb GABAergic neurons, we employed rAAV-VGAT1-hM3D(Gq)-mCherry-WPRE-pA (VGAT1-hM3Dq, AAV2/9, 5.25 × 10^{12} vg/mL, 100 nL) for activation and rAAV-VGAT1-hM4D(Gi)-mCherry-WPRE-pA (VGAT1-hM4Di, AAV2/9, 5.15 × 10^{12} vg/mL, 100 nL) for suppression, using identical LHb coordinates. Additionally, to modulate pPVT neurons, rAAV-Ef1α-CaMKIIα-hM3D(Gq)-mCherry-WPRE-pA (AAV-CaMKIIα-hM3Dq-mCherry, AAV2/9, 5.25 × 10^{12} vg/mL, 150 nL) was used for activation, and rAAV-Ef1α-CaMKIIα-hM4D(Gi)-mCherry-WPRE-pA (AAV-CaMKIIα-hM4Di-mCherry, AAV2/9, 5.11 × 10^{12} vg/mL, 150 nL) for suppression, with injections angled at 10° (AP −1.62 mm; ML 0.55 mm; DV −3.6 mm in C57BL/6J mice). After a 3-wk viral expression period, subjects received either clozapine-N-oxide (CNO, 2.5 mg/kg, i.p., from Sigma) or saline 45 min before experiments. Postviral injection (2 wk later), mice were anesthetized (1.25% avertin, 0.6 mL/20 g, i.p., from Aladdin), and a cannula (O.D. 0.2 mm/M3.5, RWD) was stereotaxically positioned into the pPVT (AP −1.62 mm; ML 0.55 mm; DV 3.1 mm) at a 10° angle and secured with dental adhesive. A recovery period of 6 d was allowed before behavioral assessments. Pretest conditioning involved handling the mice in the experimenter's gloved hands for 15 min, repeated over 2 d. For the final intervention, mice under isoflurane sedation received 100 nL injections of either 3 μM CNO, PBS, or 2 μM bicuculline in the pPVT at 50 nL/min. Behavioral assessments were conducted 5 min after the mice regained consciousness.

In Vivo Optogenetic Manipulations. For optogenetic activation of LHb GABAergic neurons in GAD2-Cre mice, rAAV-Ef1α-DIO-hChR2(H134R)-mCherry-WPRE-pA (AAV-DIO-ChR2-mCherry, AAV2/9, 5.06 × 10^{12} vg/mL, 150 nlL) was bilaterally infused into the LHb using established coordinates. The control group received rAAV-Ef1α-DIO-mCherry-WPRE-pA (AAV-DIO-mCherry, AAV2/9, 5.21 × 10^{12} vg/mL, 150 nL). In C57BL/6J mice, bilateral LHb stimulation of glutamatergic neurons was achieved using AAV-Ef1α-CaMKIIα-hChR2(H134R)-EYFP-WPRE-pA (AAV-CaMKIIα-ChR2-EYFP, AAV2/9, 5.16 × 10^{12} vg/mL, 150 nL), with AAV-Ef1α-CaMKIIα-EYFP-WPRE-pA serving as the control. Post a 2-wk viral expression period, mice were anesthetized with 1.25% avertin (0.6 mL/20 g, i.p.) and secured in a stereotaxic apparatus. An optical fiber cannula (1.25 mm diameter; 4 mm length, ThinkerTech) was accurately positioned over the LHb at coordinates AP −1.62 mm, ML 0 mm, DV −2.5 mm, and secured using dental adhesive. After a recovery period of 7 d, each mouse was habituated to the implantable optical fiber for 30 min daily over 2 d within the experimental setup. The optical fiber was connected to a ThinkerTech laser system, delivering blue light pulses (473 nm, 3 to 5 mw, 20 ms pulse width, 20 Hz) controlled by a LP-10 laser power meter (Sanwa). During the von Frey test, light stimulation was applied for 1 min, repeated five times. For the acetone test, the stimulation lasted 2 min. In behavioral tests like the OFT and EPM, the protocol followed a sequence of 3 min off, 3 min on, and 3 min off.

In Vivo Pharmacological Intervention. Subjects were anesthetized with 1.25% avertin (0.6 mL/20 g, i.p., Aladdin) and secured in a stereotaxic apparatus. A precision cannula (O.D. 0.41 mm, I.D. 0.25 mm, C.C0.8/B7.8/M3.5, RWD) was bilaterally positioned within the LHb using coordinates AP −1.62 mm, ML ±0.45 mm, and DV −2.35 mm, and secured with dental adhesive. β-sitosterol (β-sito, 1 mM, from MCE) or a control solution (10% ethanol, 90% PBS) was administered at a flow rate of 50 nL/min, delivering 100 nL per hemisphere. Behavioral assessments commenced 5 min after injection, once the mouse had recovered from anesthesia. For systemic interventions, β-sitosterol was administered intraperitoneally to pT-ION mice at doses of 10 mg/kg, 30 mg/kg, and 100 mg/kg on day 21 postsurgery. Acetone sensitivity and rotarod performance were evaluated 1 h postadministration. Behavioral assessments in the OFT and EPM were conducted 1 h after β-sitosterol or vehicle (corn oil) administration on days 23 and 25, respectively.

Anterograde Tracing. Mice were immobilized on a stereotaxic frame (RWD) and anesthetized using 1.25% avertin (0.6 mL/20 g, i.p., Aladdin). Using a Hamilton 2.5 μL microsyringe coupled with a Stoelting infusion pump, viral solutions (100 to 200 nL, adjusted based on desired expression levels and viral concentrations) were administered into predetermined brain areas at a controlled rate of 50 nL/min. The stereotactic coordinates, referenced from bregma, were as follows: anterior–posterior (AP) −1.62 mm, medio-lateral (ML) −0.45 mm, and dorso-ventral (DV) −2.85 mm. For anterograde tracing, rAAV-Ef1α-DIO-mCherry-WPRE-pA (AAV-DIO-mCherry, AAV2/9, 5.21 × 10^{12} vg/mL, 150 nL) was precisely injected into the left LHb of GAD2-Cre mice. Four weeks postinjection, the extensive distribution of the mCherry protein was verified through detailed brain imaging, indicating successful viral expression and neuronal labeling.

In Vitro Electrophysiological Recordings.

Slice preparation. Mice were killed via cervical dislocation, and brains were immediately immersed in ice-cold, oxygenated slicing solution. Coronal slices (300 μm) encompassing the LHb and pPVT regions were prepared with a Leica VT1200S vibrating microtome. The slicing solution contained (in mM): NMDG 93, KCl 2.5, NaH_2PO4 1.2, $NaHCO_3$ 30, HEPES 20, glucose 25, thiourea 2, Na-ascorbate 5, Na-pyruvate 3, $CaCl_2$ 0.5, $MgSO_4$ 10, glutathione 3, pH 7.3 to 7.4. Slices were initially incubated at 32 °C for 15 min in an oxygenated solution and then acclimated at room temperature (25 °C) for 60 min before recordings.

Whole-cell patch-clamp recordings. Recordings were conducted under an Olympus BX51WI microscope with a 40× water-immersion lens. LHb GABAergic neurons were identified by their fluorescence at 594 nm. Patch pipettes (6 to 10 MΩ), pulled from borosilicate glass, were used to record from neurons. A Multiclamp 700B amplifier processed the signals, with data analyzed using Clampfit 10.4. For sEPSCs, neurons held at −70 mV were exposed to 20 μM bicuculline to block GABAA receptors. Action potentials were elicited with current steps from −20 to +50 pA in current clamp mode. The internal pipette solution comprised (in mM): K-gluconate 125, EGTA 0.5, HEPES 10, KCl 15, Na2-phosphocreatine 10, Mg-ATP 2, Na-GTP 0.5, pH 7.3 to 7.4.

Optogenetically evoked responses. For optogenetic stimulations, neurons held at −70 mV for EPSCs or 0 mV for IPSCs were exposed to 1 s pulses of blue light (473 nm, 60 μw, 20 ms at 20 Hz). The Cs-based intracellular solution for these recordings contained (in mM): Cs-methanesulfonate 100, NaCl 10, TEA-Cl 10, $MgCl_2$ 1, EGTA 10, HEPES 30, Mg-ATP 3, Na-GTP 0.3, QX-314 4, pH 7.3-7.4.

β-sitosterol bath application recordings. β-Sitosterol (1 mM) and the ESRα antagonist AZD9496 (0.1 μM) were intermittently added to the recording bath. Following a baseline recording, β-sitosterol was applied, washed out, and reapplied with AZD9496. Effects were monitored in real-time during current-evoked firings, documenting changes in neuronal excitability postapplication.

Immunofluorescence Staining. Mice were deeply anesthetized with sodium pentobarbital (100 mg/kg, i.p., Aladdin) and perfused with saline followed by 4% paraformaldehyde. Brains were extracted and postfixed overnight in 4% paraformaldehyde at 4 °C. Tissues were then cryoprotected in 30% sucrose for 7 d before being sectioned coronally at 30 μm using a Leica 2000 cryostat. Sections underwent three 15-min washes in PBS containing 0.3% Triton X-100 to permeabilize

the tissue. Slides were then mounted with coverslips using DAPI Fluoromount-G® (Southern Biotech) for nuclear staining. To map the distribution of GABAergic neurons throughout the pPVT, brain slices were first blocked for 2 h at room temperature. They were then incubated overnight at 4 °C with rabbit anti-GAD65/67 antibodies (diluted 1:100, Abcam). Following this, the slices were thoroughly rinsed to remove unbound primary antibodies and subsequently incubated for 2 h with Alexa Fluor 488-conjugated secondary antibodies (diluted 1:1,000; Invitrogen) to enable visualization. Images were acquired with an Olympus VS120 slide scanning microscopy system, ensuring high-resolution capture of the fluorescent signals.

Statistical Analysis. Detailed descriptions of the statistical methods employed, including the statistical tests used, *P* values, sample sizes, degrees of freedom, and *t* or *F* values, are provided in the figure legends accompanying the results. Sample sizes were determined based on historical data and studies cited within relevant literature (7, 16, 23). All data are reported as mean ± SEM. Statistical significance was defined at $*P < 0.05$, $**P < 0.01$, and $***P < 0.001$ levels. Pairwise comparisons between experimental groups were conducted using a two-tailed Student's *t* test (unpaired). For analyses involving multiple comparisons, either one-way or two-way ANOVA was applied, followed by appropriate post hoc tests to correct for multiple testing. All statistical analyses and graphical representations were performed using GraphPad Prism version 8 (GraphPad Software, Inc).

Data, Materials, and Software Availability. All raw data supporting the findings of this study have been deposited in Figshare and are accessible at https://doi.org/10.6084/m9.figshare.27307590.v1 (47). All study data are included in the article and/or *SI Appendix*.

ACKNOWLEDGMENTS. We sincerely thank Prof. Yan-Gang Sun from the Chinese Academy of Sciences and Prof. Qiufu Ma from Westlake University for their invaluable guidance and insightful suggestions on the manuscript. This work was supported by the National Natural Science Funds of China (82471243, 82474629, 81971056, 82271258, 82271248, and 82204830), Zhongshan-Fudan Joint Innovation Center, Zhongshan, Guangdong Province, China (528437), the Innovative Research Team of High-level Local Universities in Shanghai, the Shanghai Municipal Science and Technology Major Project (No.2018SHZDZX01), ZJLab, and the Shanghai Center for Brain Science and Brain-Inspired Technology.

1. S. Jarrin *et al.*, Optogenetics and its application in pain and anxiety research. *Neurosci. Biobehav. Rev.* **105**, 200–211 (2019).
2. T. Chen *et al.*, Current understanding of the neural circuitry in the comorbidity of chronic pain and anxiety. *Neural Plast.* **2022**, 4217593 (2022).
3. D. Borsook *et al.*, Reward deficiency and anti-reward in pain chronification. *Neurosci. Biobehav. Rev.* **68**, 282–297 (2016).
4. L. Dou *et al.*, The prevalence of dental anxiety and its association with pain and other variables among adult patients with irreversible pulpitis. *BMC Oral Health* **18**, 101 (2018).
5. G. Lucchetti *et al.*, Anxiety and fear-avoidance in musculoskeletal pain. *Curr. Pain Headache Rep.* **16**, 399–406 (2012).
6. Y. Yang *et al.*, Ketamine blocks bursting in the lateral habenula to rapidly relieve depression. *Nature* **554**, 317–322 (2018).
7. W. Q. Cui *et al.*, Tacr3 in the lateral habenula differentially regulates orofacial allodynia and anxiety-like behaviors in a mouse model of trigeminal neuralgia. *Acta Neuropathol. Commun.* **8**, 44 (2020).
8. M. E. Flanigan *et al.*, Orexin signaling in GABAergic lateral habenula neurons modulates aggressive behavior in male mice. *Nat. Neurosci.* **23**, 638–650 (2020).
9. L. Zhang *et al.*, A GABAergic cell type in the lateral habenula links hypothalamic homeostatic and midbrain motivation circuits with sex steroid signaling. *Transl. Psychiatry* **8**, 50 (2018).
10. L. Zhang *et al.*, Thirst is associated with suppression of habenula output and active stress coping: Is there a role for a non-canonical vasopressin-glutamate pathway? *Front. Neural Circuits* **10**, 13 (2016).
11. H. Pang *et al.*, Low back pain and osteoarthritis pain: A perspective of estrogen. *Bone Res.* **11**, 42 (2023).
12. J. Ryan, M. L. Ancelin, Polymorphisms of estrogen receptors and risk of depression: Therapeutic implications. *Drugs* **72**, 1725–1738 (2012).
13. J. L. Gordon *et al.*, Ovarian hormone fluctuation, neurosteroids, and HPA axis dysregulation in perimenopausal depression: A novel heuristic model. *Am. J. Psychiatry* **172**, 227–236 (2015).
14. S. F. Rosen *et al.*, T-cell mediation of pregnancy analgesia affecting chronic pain in mice. *J. Neurosci.* **37**, 9819–9827 (2017).
15. L. Tiranini *et al.*, Is now the time to reconsider risks, benefits, and limitations of estrogen preparations as a treatment for menstrually related migraine? *Expert Rev. Neurother.* **23**, 377–388 (2023).
16. S. A. Nirmal, S. C. Pal, S. C. Mandal, A. N. Patil, Analgesic and anti-inflammatory activity of β-sitosterol isolated from Nyctanthes arbortristis leaves. *Inflammopharmacology* **20**, 219–224 (2012).
17. N. Panayotis *et al.*, Beta-sitosterol reduces anxiety and synergizes with established anxiolytic drugs in mice. *Cell Rep. Med.* **2**, 100281 (2021).
18. D. Zhao *et al.*, Structural features and potent antidepressant effects of total sterols and beta-sitosterol extracted from *Sargassum horneri*. *Mar. Drugs* **14**, 123 (2016).
19. Y. Shima *et al.*, Distinctiveness and continuity in transcriptome and connectivity in the anterior–posterior axis of the paraventricular nucleus of the thalamus. *Cell Rep.* **42**, 113309 (2023).
20. G. J. Kirouac, Placing the paraventricular nucleus of the thalamus within the brain circuits that control behavior. *Neurosci. Biobehav. Rev.* **56**, 315–329 (2015).
21. S. Ren *et al.*, The paraventricular thalamus is a critical thalamic area for wakefulness. *Science* **362**, 429–434 (2018).
22. W. Zhou *et al.*, A neural circuit for comorbid depressive symptoms in chronic pain. *Nat. Neurosci.* **22**, 1649–1658 (2019).
23. L. Huang *et al.*, A visual circuit related to habenula underlies the antidepressive effects of light therapy. *Neuron* **102**, 128–142.e128 (2019).
24. A. Sharma, A. Ghosh, E. T. Hansen, J. M. Newman, R. R. Mohan, Transduction efficiency of AAV 2/6, 2/8 and 2/9 vectors for delivering genes in human corneal fibroblasts. *Brain Res. Bull.* **81**, 273–278 (2010).
25. M. J. Castle, Z. T. Gershenson, A. R. Giles, E. L. Holzbaur, J. H. Wolfe, Adeno-associated virus serotypes 1, 8, and 9 share conserved mechanisms for anterograde and retrograde axonal transport. *Hum. Gene Ther.* **25**, 705–720 (2014).
26. D. F. Aschauer, S. Kreuz, S. Rumpel, Analysis of transduction efficiency, tropism and axonal transport of AAV serotypes 1, 2, 5, 6, 8 and 9 in the mouse brain. *PLoS ONE* **8**, e76310 (2013).
27. T. He *et al.*, The influence of murine genetic background in adeno-associated virus transduction of the mouse brain. *Hum. Gene Ther. Clin. Dev.* **30**, 169–181 (2019).
28. D. Zhao *et al.*, The altered sensitivity of acute stress induced anxiety-related behaviors by modulating insular cortex-paraventricular thalamus-bed nucleus of the stria terminalis neural circuit. *Neurobiol. Dis.* **174**, 105890 (2022).
29. W. Heydendael *et al.*, Orexins/hypocretins act in the posterior paraventricular thalamic nucleus during repeated stress to regulate facilitation to novel stress. *Endocrinology* **152**, 4738–4752 (2011).
30. W. W. Zhang *et al.*, Tachykinin receptor 3 in the lateral habenula alleviates pain and anxiety comorbidity in mice. *Front. Immunol.* **14**, 1049739 (2023).
31. V. Neugebauer *et al.*, Amygdala, neuropeptides, and chronic pain-related affective behaviors. *Neuropharmacology* **170**, 108052 (2020).
32. S. H. Liang *et al.*, A neural circuit from thalamic paraventricular nucleus to central amygdala for the facilitation of neuropathic pain. *J. Neurosci.* **40**, 7837–7854 (2020).
33. L. Xie *et al.*, Divergent modulation of pain and anxiety by GABAergic neurons in the ventrolateral periaqueductal gray and dorsal raphe. *Neuropsychopharmacology* **48**, 1509–1519 (2023).
34. J. Deng *et al.*, Distinct thalamo-subcortical circuits underlie painful behavior and depression-like behavior following nerve injury. *Adv. Sci.* **11**, e2401855 (2024).
35. H. Huang, X. Liu, L. Wang, F. Wang, Whole-brain connections of glutamatergic neurons in the mouse lateral habenula in both sexes. *Biol. Sex Differ.* **15**, 37 (2024).
36. R. Kuner, T. Kuner, Cellular circuits in the brain and their modulation in acute and chronic pain. *Physiol. Rev.* **101**, 213–258 (2021).
37. L. Shelton, L. Becerra, D. Borsook, Unmasking the mysteries of the habenula in pain and analgesia. *Prog. Neurobiol.* **96**, 208–219 (2012).
38. Y. Li *et al.*, Role of the lateral habenula in pain-associated depression. *Front. Behav. Neurosci.* **11**, 31 (2017).
39. K. Ozasa *et al.*, Association between anxiety and descending pain modulation of thermal stimuli in patients with burning mouth syndrome: A cross-sectional study. *J. Oral Facial Pain Headache* **36**, 67–77 (2022).
40. K. Nakamura, K. Wong-Lin, Functions and computational principles of serotonergic and related systems at multiple scales. *Front. Integr. Neurosci.* **8**, 23 (2014).
41. A. D. Abraham *et al.*, Estrogen regulation of GRK2 inactivates kappa opioid receptor signaling mediating analgesia, but not aversion. *J. Neurosci.* **38**, 8031–8043 (2018).
42. K. Meyer, V. Korz, Estrogen receptor α functions in the regulation of motivation and spatial cognition in young male rats. *PLoS ONE* **8**, e79303 (2013).
43. G. Bruno, V. W. Melody, B. Robert, T. Jessica, Regulation of neural gene expression by estrogen receptor alpha. bioRxiv [Preprint] (2020). 10.1101/2020.10.21.349290. (Accessed 20 September 2023).
44. S. Babu, S. Jayaraman, An update on beta-sitosterol: A potential herbal nutraceutical for diabetic management. *Biomed. Pharmacother.* **131**, 110702 (2020).
45. C. K. Wagner, A. J. Silverman, J. I. Morrell, Evidence for estrogen receptor in cell nuclei and axon terminals within the lateral habenula of the rat: Regulation during pregnancy. *J. Comp. Neurol.* **392**, 330–342 (1998).
46. P. J. Shughrue, M. V. Lane, I. Merchenthaler, Comparative distribution of estrogen receptor-alpha and -beta mRNA in the rat central nervous system. *J. Comp. Neurol.* **388**, 507–525 (1997).
47. T. Chen *et al.*, Dataset for manuscript "Differential modulation of pain and associated anxiety by GABAergic neuronal circuits in the lateral habenula. figshare. https://doi.org/10.6084/m9.figshare.27307590.v1. Deposited 25 October 2024.